Protonation of the Copper(I) Form of the Blue Copper Proteins Plastocyanin and Amicyanin – A Molecular Dynamics Study

Christian Buning[a] and Peter Comba*[a]

Keywords: Blue copper proteins / Molecular dynamics / Cluster analysis / Protonated histidine / Protonation mechanism

The conformational space of the copper(I) forms of the cupredoxines amicyanin (ami) (*Paracoccus versutus*) and plastocyanin (pla) (*Populus nigra*) with a protonated histidine donor close to the C-terminus ("C-terminal histidine" ami: His96; pla: His87) was investigated with force field calculations that involve the experimentally determined structures of the protonated or unprotonated copper(I/II) forms: a setup of 36 conformers with a constrained torsional angle that involves the $C_{imidazole}$–$C_{methylene}$ (C^{γ}–C^{β}) bond (chi2; 10° increments); strain energy minimization of all constrained conformers; a 10 ps molecular dynamics search around each conformer; constrained, followed by unconstrained optimization of each of the resulting low energy structures; cluster analysis of the resulting conformations. For both cupredoxines there are two major conformers which differ in their solvent accessibility. The plastocyanin and amicyanin structures are in excellent agreement with the experimentally observed crystallographic data; the two analyses lead to the proposal for a general mechanism for the protonation of reduced blue copper proteins. This is also in agreement with the results of a conformational analysis of a complex of the protonated copper(I) form of amicyanin with phosphate.

Introduction

Blue copper proteins (cupredoxines) are relatively small metalloproteins (approximately 10–14 kDa, 100–150 amino acid residues) with a single copper center in a trigonal pyramidal coordination geometry (two histidines, a cysteine, and an axial methionine; type 1 copper center). Cupredoxines are one-electron transfer centers which are part of redox chains in plants and bacteria.[1] Among the most prominent properties are the typical intense blue color in the oxidized form [ε (≈600 nm) ≈ 5000 $L \cdot mol^{-1}cm^{-1}$; proteins with rhombic sites have increasing intensity of a second transition at ≈460 nm], attributed to charge transfer from the cysteinate donor, a small A_z hyperfine coupling in the EPR spectrum ($A_z \approx 50 \cdot 10^{-4}$ cm^{-1}), relatively high reduction potentials [≈200 to ≈680 mV vs. 150 mV for the aqueous copper(II/I) couple] and fast electron self-exchange rates [10^3 to 10^6 $M^{-1}s^{-1}$ vs. $5 \cdot 10^{-7}$ $M^{-1}s^{-1}$ for the aqueous copper(II/I) couple].[2–5] A plot of the structure of amicyanin from *Paracoccus versutus* is shown in Figure 1.

An interesting feature is that for some of the blue copper proteins the reduction potential is strongly pH-dependent, and this has been attributed to the protonation of the coordinating histidine residue close to the C-terminus ("C-terminal histidine"; His96 in amicyanin shown in Figure 1). This histidine is supposed to be the gate for electron transfer, and protonation/deprotonation (i.e. bond breakage/bond formation may then be a switch to turn off and on the electron transfer reactivity.[6]). There is experimental

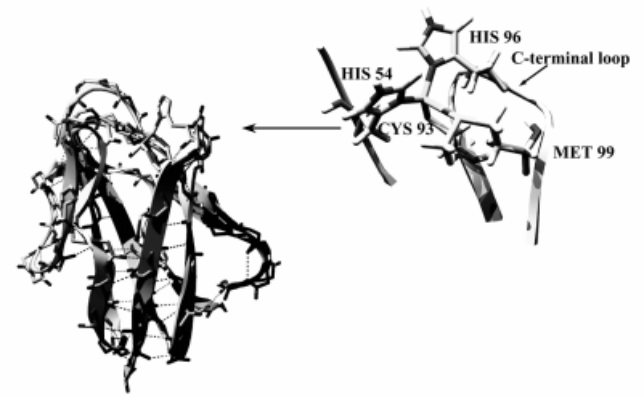

Figure 1. Representation of the tertiary structure and of the copper chromophore of amicyanin (*Paracoccus versutus*)[23]

electrochemical evidence for this protonation in plastocyanin, pseudoazurin, and amicyanin.[6–9] Structural support for the protonation has been obtained from X-ray studies of plastocyanin, pseudoazurin, and amicyanin.[10–12] [see Figure 2 for plastocyanin (His87)].

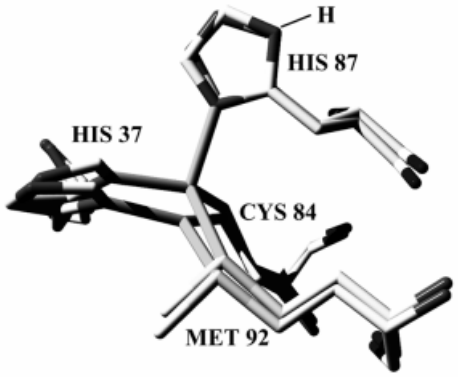

Figure 2. Overlay of the protonated and the unprotonated Cu^{I}-structures of plastocyanin[11]

[a] Anorganisch Chemisches Institut der Universität Heidelberg, Im Neuenheimer Feld 270, 69120 Heidelberg, Germany, Fax: (internat.) +49–6221/54-6617
E-mail: comba@akcomba.oci.uni-heidelberg.de

Supporting information for this article is available on the WWW under http://www.wiley-vch.de/home/eurjic or from the author.

  1434–1948/00/0606–1267 $ 17.50+.50/0

There are two known structures for the protonated copper(I) form of plastocyanin.[11] The major difference is the conformation of the corresponding histidine side chain. One of the structures has the protonated N^{δ} directed towards the copper center whereas in the other structure the residue is rotated around chi2 by 180° (see Table 1 for nomenclature of the torsional angles), so that the protonated N^{δ} becomes solvent accessible and forms a hydrogen bond with a water molecule. During the protonation the geometry around the copper center changes from trigonal pyramidal to trigonal planar (see Figure 2). The distance to S^{δ} from the methionine decreases from 2.9 Å to 2.5 Å in the trigonal planar form, the bond distances to S^{γ} from the cysteine and to N^{δ} from the histidine do not change significantly. The trigonal planar geometry as well as the presence of two soft donors disfavors the copper(II) oxidation state, and this leads to the observed increase of the reduction potential.

Table 1. Definition of the torsion angles

Torsion	Atom type			
ϕ	C	C^{α}	N	C
Ψ	N	C	C^{α}	N
Ω	C^{α}	N	C	C^{α}
$\chi 1$	N	C^{α}	C^{β}	C^{γ}
$\chi 2$	C^{α}	C^{β}	C^{γ}	$N^{\delta 1}$
Tor	C^{α}	C^{β}	C^{γ}	$C^{\delta 2}$

For amicyanin there are detailed kinetic studies, suggesting that two protonated forms (His96) with different structures are involved[6] (Scheme 1). The rearrangement (k_2) is slow compared to the protonation (k_1). The observed pK_a value depends on the phosphate ion concentration, suggesting that some phosphate coordination is involved. Structural information on the protonated forms is available from an EXAFS study of amicyanin at variable pH.[13] This indicates the loss of one histidine donor at low pH and a reorganization of the copper site towards a trigonal planar geometry. There are also recent X-ray studies of the protonated form of amicyanin.[10] These indicate that, for amicyanin, there are two conformers for the protonated side chain of the C-terminal histidine.

$$A \underset{k_{-1}}{\overset{[H^+]\ k_1}{\rightleftharpoons}} B \underset{k_{-2}}{\overset{k_2}{\rightleftharpoons}} C$$

Scheme 1. Three site exchange equilibrium describing the protonation of Cu^{I}-amicyanin

A pH-dependent electrochemical study of azurin (*Pseudomonas aeruginosa*) indicates that, in this cupredoxine, the coordinating histidine residues may not be protonated.[14–16] Factors that might prevent protonation are: (i) the length of the C-terminal loop: based on the observation that only those wildtype cupredoxines protonate which have two spacing amino acids between the Cys and the His[7] it was suggested that the length of the C-terminal loop is the determining factor for the protonation; (ii) the presence of the sterically demanding side chain Phe114 (azurin) in close proximity to the C-terminal His might prevent the rotation around chi2;[2,17] (iii) the absence of a proline residue next to the C-terminal His (Pro95 in amicyanin):[2,7,18] for all wildtype cupredoxines that protonate there is a Pro residue in the i-1 position with respect to the C-terminal histidine; this proline is known to interact with the protonated His of plastocyanin.[11] Recent loop-mutation studies yielded an amicyanin mutant with an azurin C-terminal loop (AmiAzu), where the coordinating C-terminal histidine may be protonated in the copper(I) form.[19] This mutant is the first cupredoxine which undergoes a protonation of the C-terminal histidine and which has more than two noncoordinating amino acids between the Cys and His donors in the C-terminal loop and no proline residue in the i-1 position which might interact with the protonated histidine side chain.

We have used molecular dynamics calculations to analyze the structural details of the protonated copper(I) forms of two blue copper proteins, plastocyanin and amicyanin, which are known to have protonated coordinating histidine groups (His96, pK_a = 6.8; His87, pK_a = 4.7, respectively). The results of the two MD calculations were also used to propose a detailed, general mechanism for the protonation of reduced cupredoxines. For amicyanin, an MD calculation of an amicyanin/phosphate complex was used to model the phosphate-dependence of the proton transfer reaction.

Computational Details

Force Field and Structural Models

DISCOVER 2.9.5.[20] with the force field AMBER[21] was used for all MM and MD calculations. The chromophore [copper(I) center and the three donor atoms of the coordinated amino acid residues (S, S, N)], the protein backbone outside a shell with a radius of 10 Å around C^{γ} of the C-terminal histidine (see Table 2), on the basis of entire amino acid residues, and the water molecules outside a shell with a radius of 7 Å were held at fixed positions. A distance-

Table 2. Amino acid sequences of the C-terminal loops of several blue copper proteins

Protein	Origin	Sequence of the C-terminal loop										
Amicyanin	*Paracoccus versutus*	**Cys**	Thr	Pro			**His**	Pro	Phe			**Met**
Plastocyanin	*Populus nigra*	**Cys**	Ser	Pro			**His**	Gln	Gly	Ala	Gly	**Met**
Pseudoazurin	*Alcaligenes faecalis*	**Cys**	Thr	Pro			**His**	Tyr	Ala	Met	Gly	**Met**
Azurin	*Pseudomonas aeroginosa*	**Cys**	Thr	Phe	Pro	Gly	**His**	Ser	Ala	Leu		**Met**

dependent dielectric constant ($\varepsilon = 1 \times r$) and a cutoff of 12 Å for the nonbonded interactions were used. The point charges were those of the AMBER force field,[21] except for the copper(I) chromophore, where the charge distribution was computed with GAUSSIAN94.[22] [Merz-Kollmann scheme; B3LYP, Dζpdf/6-31G* basis set; model compound: $Cu^{I}(SCH_3)\{S(CH_3)_2\}(Im)$ with experimental coordinates of copper(I) plastocyanin, PDB-code 6pcy[11]]. The parameters for the chromophore are [copper(I) was treated as a cation, i.e. no bonds to the donor atoms; point charge, R, ε]: Cu^{I}, 0.118, 2.4, 0.05; S_{cys}, –0.546, 4.0, 0.2; N_{His}, –0.163, 3.5, 0.16. The point charges of the entire model compound are given as supplementary material.

Conformations of the Protonated Copper(I) Form of Plastocyanin and Amicyanin

The starting structures for the conformational searches were based on experimentally determined crystallographic data; plastocyanin: *Populus nigra*, copper(I) pH = 3.8; PDB-code 6pcy;[11] amicyanin: *Paracoccus versutus*, copper(II) form;[23] the trigonal copper(I) chromophore of amicyanin was set up from this structure, based on published EXAFS data:[13] $d_{Cu–S(Cys)}$ = 2.18 Å, $d_{Cu–S(Met)}$ = 2.41 Å, $d_{Cu–N(His)}$ = 1.89 Å; assigned pH = 5.5. The copper chromophores were constrained to the experimentally observed geometries in all MD calculations. The experimentally observed water molecules were deleted from the structural data files and a solvation shell with a radius of 17 Å around C^{γ} of the C-terminal histidine (see Table 2) was constructed with a simple point charge model (SPC).

A set of 36 structures for each of the two protonated copper(I) proteins was created by a variation (10° increments) of the C^{α}–C^{β}–C^{γ}–C^{δ} torsional angle (tor) of the C-terminal histidine (see Table 1). The resulting structures were optimized (constrained angle tor, 1000 cycles, steepest descent). A 10 ps MD simulation was then performed for each of these structures (constrained angle tor, T = 600 K, 10 structures each were collected). During the MD simulation the temperature was regulated with a temperature relaxation time τ of 0.1 ps. In all calculations a time step of 1 fs was used.[24] The resulting 360 structures for each of the two copper proteins were then optimized with a constrained angle tor (10000 cycles conjugate gradient), followed by a full optimization without constraints (10000 cycles conjugate gradient).

A cluster analysis was performed for the fully energy minimized structures. The protein backbone torsions of the C-terminal loop and the side chain torsions of the protonated histidine were taken as criteria for the clustering; plastocyanin: chi1/chi2 His87, phi/psi Ala90, phi/psi Gly89, chi1/chi2 Pro86, and phi/psi Gly91; amicyanin: chi1/chi2 His96, phi/psi His96, chi1/chi2 Pro95, chi1/chi2 Pro97, and phi/psi Met99 (see Table 1 for the definition of the torsional angles and Table 2 for the amino acid sequences of the C-terminal loops of plastocyanin and amicyanin). A clustering according to these torsions allowed the definition of 12 families for amicyanin and 21 families for plastocyanin (only the highest populated clusters were examined in detail; the assignment to a cluster was based on a graphical analysis of the corresponding phi/psi plots and chi1/chi2 plots, respectively).

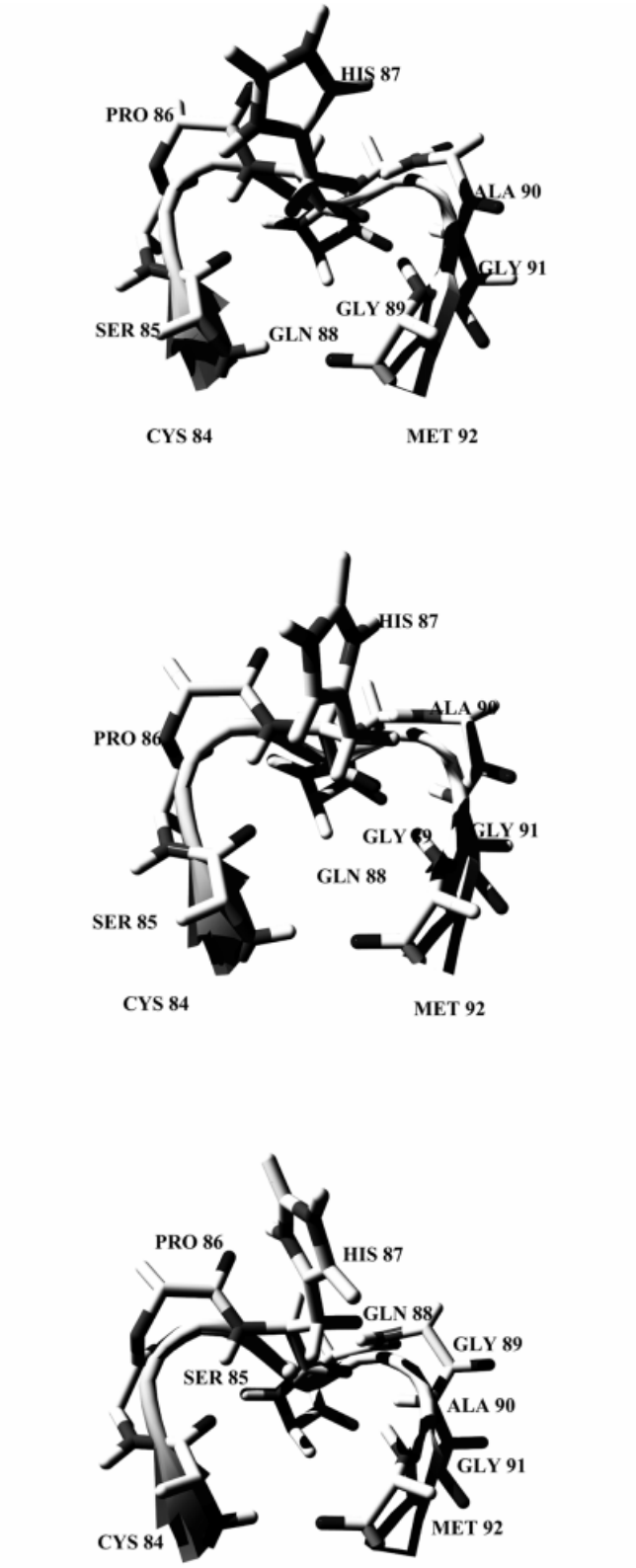

Figure 3. Representatives of the determined plastocyanin cluster: plasto1 (*top*), plasto2 (*middle*), plasto3 (*bottom*). The protein backbone of the C-terminal loop is shown plus the side chain of His 87

The Amicyanin Phosphate Complex

The structure of the protonated copper(I) amicyanin, as defined above, was used as the starting structure. Hydrogenphosphate was put in a position favorable for hydrogen bonding to N^{δ} of His96 and N–H of Arg100. The hydrogen bonds were constrained to a value of 2.5 Å. This model was energy-minimized using 10000 steps of conjugate gradient. An MD simulation at 900 K, taking 80 ps dynamics and 15 ps equilibration time was performed (τ = 0.1 ps, time step of 1 fs, see above). 80 conformations were collected and energy-minimized, using 10000 steps of conjugate gradient.

Results and Discussion

Plastocyanin

Three clusters of plastocyanin (plasto1, plasto2, plasto3) and two of amicyanin (ami1, ami2) were identified, each of which had a high population and characteristic features with respect to the histidine side chain and the C-terminal loop conformation (details of the cluster analyses are available as Supplementary Material); representative structures of the C-terminal loops are shown in Figure 3 and Figure 4, respectively. Table 3 gives detailed information on the conformation of the C-terminal loop and the protonated histidine side chain for the computed clusters and relevant experimental structures. From a comparison of the chi1/chi2 values of the three plastocyanin clusters with experimental data from X-ray studies[11] it emerges that plasto1 is very similar to the copper(I) structure at pH = 7 (deprotonated) and plasto2 is equivalent to the structure at pH = 3.8 (protonated). For plasto3 with a chi2 value of –11° there is no corresponding experimental data, and it appears that plasto3 is an intermediate between the two experimentally observed conformations. It is interesting to note here that the results of the crystallographic study of the low pH copper(I) form of plastocyanin suggest that this could be a mixture of two different conformations.[11] Thus, plasto3 might be a

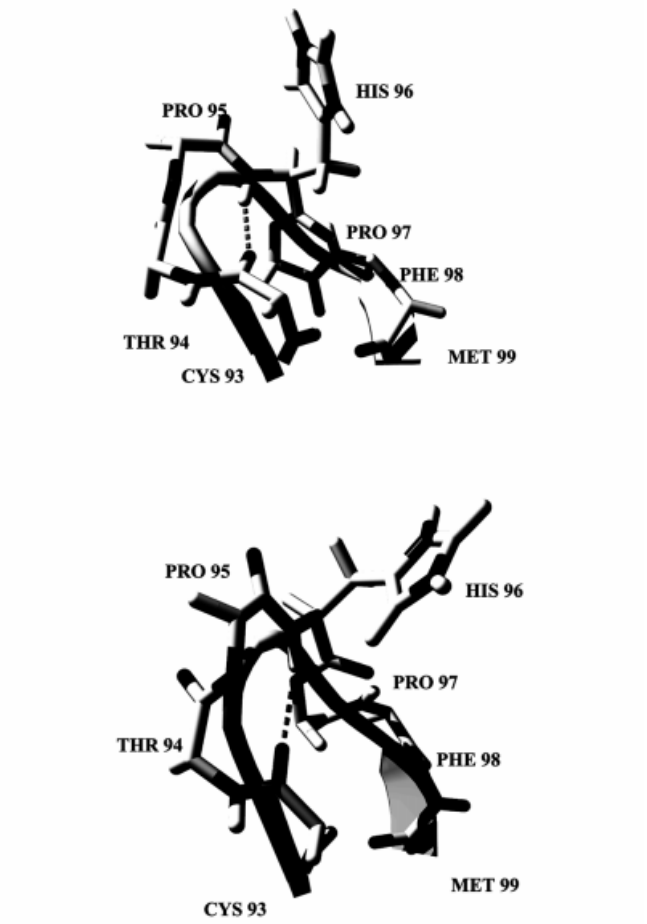

Figure 4. Representatives of the determined amicyanin cluster: ami1 (*top*), ami2 (*bottom*). The protein backbone of the C-terminal loop is shown plus the side chain of His 96 (hydrogen bonds are indicated by a dotted line)

Table 3. Comparison of the computed psi/psi torsion angles from the plastocyanin and amicyanin clusters and the chi1/chi2 angles from the protonated histidines with experimental data

		histidine	turn 1[a]		turn 2[a]		turn 3[a]	
		chi1/chi2	i+1	i+2	i+1	i+2	i+1	i+2
MD	plasto1[b]	–64°/130°	–56°/–60°	–66°/–28°	–66°/–28°	–108°/29°	–56°/–40°	–1°/–27°
MD	plasto2[b]	–59°/–71°	–61°/–47°	–48°/–40°	–48°/–40°	–117°/39°	–54°/–36°	–91°/14°
MD	plasto3[b]	–59°/–11°	–55°/–48°	–48°/–41°	–48°/–41°	–116°/25°	–55°/–37°	–87°/4°
X-ray	Plastocyanin[c]	–66°/–50°	–60°/–49°	–66°/–25°	–66°/–25°	–121°/24°	–69°/–25°	–70°/–8°
X-ray	Plastocyanin[d]	–60°/128°	–63°/–50°	–67°/–22°	–67°/–22°	–118°/14°	–67°/–29°	–70°/–8°
MD	ami1[b]	–74°/142°	–46°/–56°	–73°/–12°	–53°/–34°	–58°/–27°	–	–
MD	ami2[b]	36°/–168°	–47°/–47°	–65°/–22°	–83°/34°	–73°/–28°	–	–
X-ray	Amicyanin[e]	–49°/120°	–50°/–56°	–73°/–15°	–61°/–18°	–69°/–13°	–	–
NMR	Amicyanin[f] (A)	–	–63°/–32°	–74°/–33°	–51°/–41°	–67°/–19°	–	–
NMR	Amicyanin[f] (B)	–	–41°/107°	–2°/62°	–51°/–41°	–67°/–19°	–	–
MD	Amicyanin phosphate complex	–176°/52°	–67°/–57°	–66°/82°	–78°/57°	–100°/30°	–	–
X-ray	Pseudoazurin[g]	–52°/96°	–57°/–57°	–59°/–42°	–60°/–23°	–90°/1°	–	–

[a] Definition of the turns: plastocyanin turns 1–3: cys84-his87, ser85-gln88, gln88-gly91; amicyanin turns 1–2: cys93-his96, his96-met99; pseudoazurin turns 1–2: cys78-his81, tyr82-gly85. – [b] Median of the structures of the cluster. – [c] *Populus nigra* [Cu^{I}]; pH = 3.8 (ref.[11]). – [d] *Populus nigra* [Cu^{I}]; pH = 7 (ref.[11]). – [e] *Paracoccus versutus* [Cu^{II}] (ref.[23]). – [f] *Paracoccus versutus* [Cu^{I}] (ref.[23]). – [g] *Alcaligenes faecalis* [Cu^{I}] (ref.[12]).'

proposal for the second of these conformations at pH = 3.8.

Amicyanin

The good agreement between the computed and observed copper(I) structures of plastocyanin (see above) indicates that, based on the same MD scheme, a reasonable and accurate structural model for the protonated copper(I) form of amicyanin should be available. The cluster ami1 with a chi1/chi2 combination of –74°/142° has, in terms of the conformation of the histidine side chain, a structure that is similar to the copper(II) crystal structure.[23] In the other cluster, ami2, the protonated N^{δ} is directed towards the solvent; this conformation is similar to that of plasto2. Thus, for amicyanin there are conformations of the histidine side chain that are very similar to those of plastocyanin (see Table 3). Very recently, some experimental data on the protonated form of amicyanin became available.[10] These are in full agreement with our computed structural data.

It is instructive to extend the structural comparisons for amicyanin and plastocyanin [copper(I), unprotonated and protonated forms, experimental and computed data] to the first turn of the loop (see Table 3). A type 1 geometry is conserved in all structures. Overlay plots of all relevant structures are presented in Figure 5. The most significant structural differences for amicyanin are those of the conformations of the second turn and, for plastocyanin, those of the conformations of the third turn.

The Amicyanin/Phosphate Complex

The fact that the pK_a of amicyanin depends strongly on the phosphate anion concentration[6] suggests that an amicyanin/phosphate complex mediates the proton transfer. Published experimental data[6] indicate that the protonation rate, based on a mechanism that does not involve phosphate-protein interactions (k_1 in Scheme 1), is about two orders of magnitude faster than the diffusion-controlled limit and that, in the presence of phosphate, the proton is transferred from phosphate to the histidine nitrogen without any involvement of water molecules. A possible interpretation of these observations is that a phosphate anion binds to the positively charged Arg100 side chain. The fixed phosphate anion could then act as an anchor for protons, leading to a high local concentration. Furthermore, the Arg100-coordinated phosphate might have an ideal geometry for the stabilization of the protonated form C in Scheme 1, where the protonated N^{δ} of His96 is directed towards the solvent. There are experimental data that support a histidine/phosphate complex formation. X-ray data are available for structures which contain the motif of a phosphate or sulfate anion forming a salt bridge between a protonated histidine and a second basic amino acid.[25,26] For amicyanin, these structural and mechanistic hypotheses were examined by MD. The most favorable optimized structure of a corresponding amicyanin/phosphate complex is shown in Figure 6.

The structural model visualizes the feasibility of the discussed protonation mechanism and the stabilization of the protonated form. The hydrogen bonds between the phosphate anion and the protein are around 1.6 (± 0.1) Å (OH distances), which is at the shorter limit of the expected range. The main structural differences in the C-terminal loop of this structure, in comparison with the experimentally observed structure[23] are conformational changes at

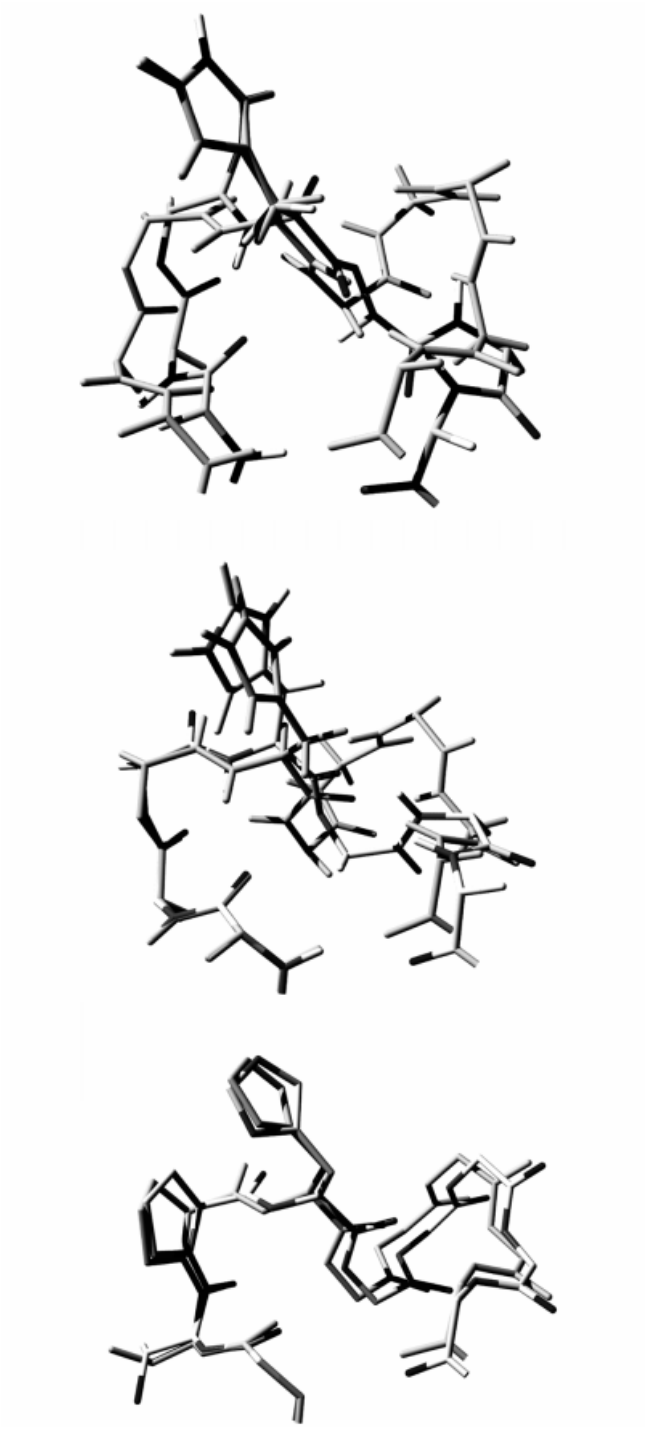

Figure 5. *Top:* Overlay of the clusters from amicyanin and plastocyanin with the protonated N^{δ} directing towards the Cu center; *middle:* Overlay of the clusters from amicyanin and plastocyanin with the N^{δ} directing into the solvent; *bottom:* Overlay of the protonated Cu^{I} structures from plastocyanin and pseudoazurin showing the protein backbone of the C-terminal loop and the side chain of the protonate histidine and the proline from the first turn

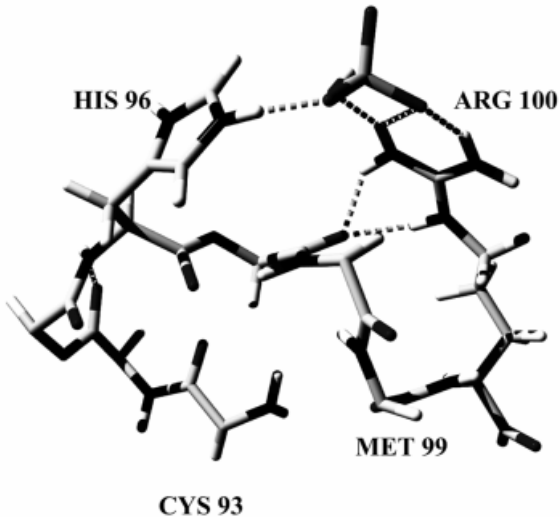

Figure 6. Calculated structure of the possible His 96-phosphate-Arg 100 complex for amicyanin from *Paracoccus versutus* (hydrogen bonds are indicated by dotted lines)

Pro95, His96, and Pro97. The conformation of His96, enforced by the coordinated phosphate anion, leads to chi1/chi2 values of –176°/52° (t/g^+). This is different from the X-ray structure of the unprotonated form[23] but one of the theoretically favored conformations (see above and Supplementary Material; g^+/g^+; g^+/g^-; t/g^+; g^-/g^+; k^-/k^-). Especially notable, however, are the phi/psi combinations for the two proline and the histidine residues (His96: 69°/100°, Pro95: –66°/82°, Pro97: –78°/57). The computed torsional angle combinations are in the ranges that are usually observed for left-handed helices (His96) or β-sheets (Pro95, Pro97), i.e., this is a reasonable conformation for the protonated C-terminal loop of the copper(I) form of amicyanin.

Conclusion

The general MD scheme used here is validated by the observation that, for plastocyanin, the experimentally observed structures are accurately reproduced. Therefore, the computed structures of the protonated copper(I) forms of amicyanin are a reliable model. The corresponding amicyanin/phosphate complex indicates how phosphate may mediate the proton transfer. All published experimental data and the computational results presented here indicate that the following steps are involved in the protonation of the C-terminal histidine in reduced blue copper proteins (see Figure 7):

(i) Decomplexation of the C-terminal histidine (structure **B**); (ii) isomerization to structure **C** with a solvent accessible histidine; (iii) protonation of the C-terminal histidine (structure **D**); (iv) isomerization to structure **E** (stabilization of the protonated structure). The rotational barrier involved in the first isomerization (**B→C**) and the solvent accessibility of structure **C** determine whether a protonation takes

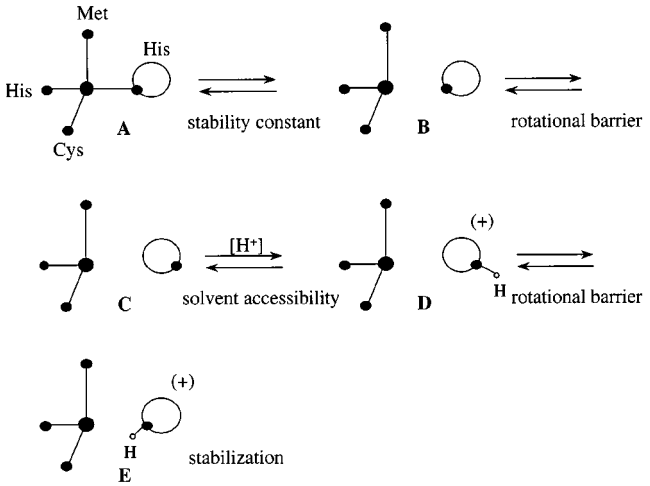

Figure 7. Schematic representation of the basic steps during the protonation of the histidine in a blue copper protein

place or not. The second rotational barrier (**D→E**) and the stabilization of structure **E** have a strong influence on the pK_a value.

Supporting Information

Details of the cluster analysis and the point charges (4 pages) are given as Supporting Information.

Acknowledgments

Generous financial support by the Volkswagen Stiftung is gratefully acknowledged. We are also grateful to Martin Frank for his help with the MD calculations and the data analyses, and to Dr. Ulf Ryde for the calculation of the point charges.

[1] C. Dennison, G. W. Canters, S. de Vries, E. Vijgenboom, R. J. van Spanning, *Adv. Inorg. Chem.* **1998**, *45*, 351–407.
[2] E. T. Adman, *Curr. Opinion Struct. Biology* **1991**, *1*, 895.
[3] G. A. Sykes, *Adv. Inorg. Chem* **1991**, *36*, 377.
[4] M. J. Sisley, R. B. Jordan, *Inorg. Chem.* **1992**, *31*, 2880–2884.
[5] P. Comba, *Coord. Chem. Rev.*, in press.
[6] A. Lommen, G. W. Canters, *J.Biol.Chem.* **1990**, 2768–2774.
[7] C. Dennison, T. Kohzuma, W. McFarlane, S. Suzuki, G. A. Sykes, *J. Chem. Soc., Chem. Commun.* **1994**, 581.
[8] C. L. Kojiro, L. Markley, *Eur. J. Biochem.* **1983**, 52–56.
[9] C. Dennison, E. Vijgenboom, W. R. Hagen, G. W. Canters, *J. Am. Chem. Soc.* **1996**, *118*, 7406–7407.
[10] Z. Zhu, L. M. Cunane, Z.-W. Chen, R. C. E. Durley, F. S. Mathews, V. L. Davidson, *Biochemistry* **1998**, *37*, 17128–17136.
[11] J. M. Guss, P. R. Harrowell, M. Murata, V. A. Norris, H. C. Freeman, *J. Mol. Biol.* **1986**, *192*, 361.
[12] E. Vakoufari, K. S. Wilson, K. Petratos, *FEBS Letters* **1994**, *347*, 203.
[13] A. Lommen, S. Wijmenga, C. W. Hilbers, G. W. Canters, *Eur. J. Biochem.* **1991**, *201*, 695.
[14] M. C. Silvestrini, M. Brunori, M. Tegoni, M. Gervais, F. Labeyrie, *Eur. J. Biochem.* **1986**, 465–472.
[15] A. F. Corin, R. Bersohn, P. E. Cole, *Biochemistry* **1983**, *22*, 2032–2038.
[16] O. Farver, Y. Blatt, I.-E. Pecht, *Biochemistry* **1982**, *21*, 3556–3561.
[17] M. V. Botuyan, A. Toy-Palmer, J. Chung, R. C. Blake II, P. Beroza, D. A. Case, H. J. Dyson, *J. Mol. Biol.* **1996**, *263*, 752.
[18] J. M. Guss, E. A. Merritt, R. P. Phizackerley, H. C. Freeman, *J. Mol. Biol.* **1996**, *262*, 686–705.

[19] C. Buning, G. W. Canters, P. Comba, C. Dennison, L. Jeuken, M. Melter, J. Sanders-Loehr, *J. Am. Chem. Soc.* **2000**, *122*, 204.
[20] *Molecular Simulations*: San Diego, California, USA.
[21] S. J. Weiner, P. A. Kollman, D. A. Case, U. C. Singh, C. Ghio, G. Alagona, S. Profeta Jr., P. Weiner, *J. Am. Chem. Soc.* **1984**, *106*, 765–784.
[22] M. J. Frisch, G. W. Trucks, A. B. Schlegel, P. M. W. Grill, B. G. Johnson, M. A. Robb, J. R. Cheeseman, T. A. Keith, G. A. Petersson, J. A. Montgomery, K. Raghavachari. M. A. Al-Laham, V. G. Zakrzcwski, J. U. Ortiz, J. B. Foresman, J. Cioslowski, B. B. Stefanov, A. Nanayakkara, C. Y. Challacombe, C. Y. Peng, P. Y. Agala, W. Chen, M. W. Wong, J. L. Andres, E. S. Replogle, R. Gomperts, R. L. Martin, D. J. Fox, J. S. Binkley, D. J. Defres, J. Baker, J. P. Stewart, M. Head-Gordon, C. Gonzales, J. A. Pople, GAUSSIAN 94, *Gaussian Inc.*, Pitsburgh, PA, **1995**.
[23] A. Romero, H. Nar, R. Huber, A. Messerschmidt, A. P. Kalverda, G. W. Canters, R. Durley, F. S. Mathews, *J. Mol. Biol.* **1994**, *236*, 1196–1211.
[24] H. J. C. Berendsen, J. P. M. Postma, W. F. van Gunsteren, A. DiNola, J. R. Haak, *J. Chem. Phys.* **1984**, *81*, 3684.
[25] E. N. Baker, *J. Mol. Biol.* **1988**, *203*, 1071.
[26] L. Chen, R. Durley, F. S. Mathews, V. L. Davidson, *Science* **1994**, 86–90.

Received September 20, 1999
[I99332]